Two-Way Pattern Grating Lobe Control for Distributed Digital Subarray Antennas

Bo-Kai Feng, *Member, IEEE*, and David C. Jenn, *Senior Member, IEEE*

***Abstract*—An approach to controlling the two-way pattern (i.e., the product of the transmitting and receiving antenna patterns) for a distributed digital subarray antenna (DDSA) is presented. Collectively combining periodic widely separated subarrays results in grating lobes (GLs), and they are unwanted because of the ambiguities that accompany them. The approach to GL control presented here involves a combination of conventional suppression methods on the transmitting side and in the digital beamforming on the receiving side, filling the gaps between the subarrays with "virtual" elements, thus forming a contiguous array. Individually, the transmitting and receiving antenna patterns may not have adequate performance, but it is demonstrated that if designed to complement each other, the two-way pattern can achieve ultralow sidelobe performance. The effects of receiving element signal-to-noise ratio (SNR) and errors in calibration are also addressed.**

***Index Terms*—Distributed subarray antennas, grating lobe (GL) suppression, two-way pattern, virtual elements.**

I. Introduction

COMPLETE digital control of amplitude and phase at the element level of an array allows great flexibility in beamforming. Modern radar and communications systems incorporate phased arrays with wider bandwidths, allowing for the possibility that several systems on the same platform can share arrays. A system that incorporates distributed digital subarrays (DDSAs) working cooperatively as a single array, thus forming an array of subarrays, can potentially increase the output signal-to-noise ratio (SNR) and provide better spatial resolution compared with using the subarrays individually.

A major factor impacting the antenna architecture is the platform design philosophy, particularly for military applications that require low signatures. It is difficult to find an available area sufficient for a large array on board a platform, so it might be necessary to use several relatively small noncontiguous (separated) areas (subarrays) and then process the received signal coherently. The technical challenges of such an approach include time and frequency synchronization, calibration, and error correction.

Manuscript received July 31, 2014; revised May 11, 2015; accepted July 09, 2015. Date of publication August 07, 2015; date of current version October 02, 2015.

B.-K. Feng is with the National Chung-Shan Institute of Science and Technology, Longtan 32546, Taiwan (e-mail: felixfeng@kiss99.com).

D. C. Jenn is with the Department of Electrical and Computer Engineering, Naval Postgraduate School Monterey, Monterey, CA 93943 USA (e-mail: jenn@nps.edu).

Color versions of one or more of the figures in this paper are available online at http://ieeexplore.ieee.org.

Digital Object Identifier 10.1109/TAP.2015.2465863

Periodically, distributed subarrays (subarrays whose centers are equally spaced) form a long baseline and are capable of very accurate angular location of targets [1], [2]. However, collectively combining periodic widely separated subarrays results in grating lobes (GLs), and they are unwanted because of the ambiguities that accompany them. Even if the individual array patterns have no GLs, conventional beamforming with periodic DDSAs will have an output response with GLs that cannot be suppressed using traditional windowing methods.

In this paper, we focus on distributed antennas that comprised subarrays that can operate individually or collectively. It is assumed that no GLs appear in the visible region for each subarray when scanned. We employ techniques for GL suppression on both the transmitting and receiving sides of the distributed array system. Individually, the transmitting and receiving antenna patterns may not have adequate performance, but if designed to complement each other, the two-way pattern (i.e., the product of the transmitting and receiving patterns) can achieve acceptable performance. Radar is the primary application of interest; however, the techniques presented can be extended to other electronic systems as well.

In Section II, the general formulas for the pattern of a DDSA with arbitrary geometry are presented, and some special cases discussed. In Section III, we summarize the conventional methods for array GL suppression. Some examples of conventional GL reduction methods that can be applied to DDSAs are discussed in Section IV. Few of these methods have been applied to distributed subarrays. Due to the limited effectiveness in suppressing DDSA GLs by these conventional methods, in Section V, we investigate a new approach which utilizes the power of digital signal processing to eliminate the GLs and further lower the sidelobes on the receiving pattern. In Section VI, it is demonstrated that a combination of the traditional methods on the transmitting side together with the digital beamforming and processing on the receiving side provide significant two-way pattern improvement. In Section VII, an analysis of the effect of calibration errors and SNR is addressed. Section VIII gives a summary and conclusion.

II. Formulas for DDSA

In Fig. 1, an illustration of the general array geometry is shown, where

N_s = number of subarrays,

m = subarray index ($m = 1, 2, \ldots, N_s$), and

$x_s(m), y_s(m), z_s(m)$ = coordinates of subarray m in the global system.

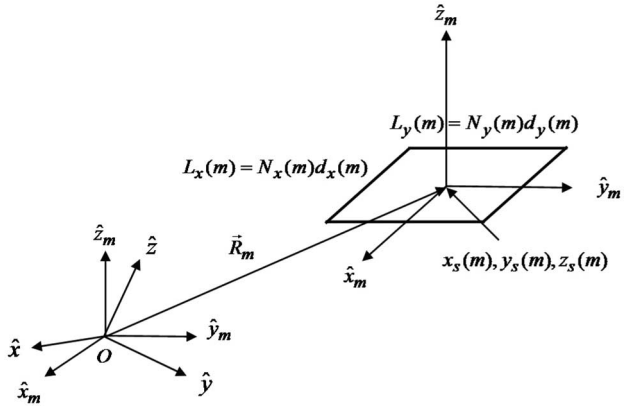

Fig. 1. Subarray m and its local coordinate system relative to the global origin.

The subarrays can be rotated and tilted with respect to the global origin. In the global system, for an observer at (θ, ϕ), the direction cosines are

$$\begin{aligned} u &= \sin\theta\ \cos\phi \\ v &= \sin\theta\ \sin\phi \\ w &= \cos\theta. \end{aligned} \tag{1}$$

Similarly, the direction cosines in the scan direction in global coordinates (θ_s, ϕ_s) can be denoted as (u_s, v_s, w_s). In the local subarray *m* coordinate system, the corresponding direction cosines of an observer at (θ_m, ϕ_m) are (u_m, v_m, w_m) and the scan angle direction cosines are denoted (u_{sm}, v_{sm}, w_{sm}). A rotation matrix can be used to obtain the subarray direction cosines from the global ones and vice versa.

Consider planar rectangular subarrays with all elements in the local $z = 0$ plane. The element spacing is constant within each subarray, but can vary from subarray to subarray. The number of elements in the subarrays can vary such that

$N_x(m), N_y(m) =$ number of elements in the local x and y directions for subarray m, and

$d_x(m), d_y(m) =$ spacing between elements for subarray m.

The complex pattern of the mth subarray is given by the sum

$$\begin{aligned} F_s(m) = &\sum_{p=1}^{N_x(m)} \sum_{q=1}^{N_y(m)} W(m,p,q) \\ &\times \exp\left[jk(x(m,p)u_m + y(m,q)v_m)\right] \end{aligned} \tag{2}$$

where $k = 2\pi/\lambda$ (λ is the wavelength at the frequency of operation and an $e^{j\omega t}$ time dependence is assumed and suppressed). The complex weight

$$W(m,p,q) = a(m,p,q)e^{j\psi(m,p,q)} \tag{3}$$

at element p, q of subarray m is applied for scanning, sidelobe control, beamshaping, and error compensation. For equally spaced elements, with each subarray centered at its local origin

$$\begin{aligned} x(m,p) &= \frac{2p - (N_x(m)+1)}{2} d_x(m) \equiv P(m,p)d_x(m) \\ y(m,q) &= \frac{2q - (N_y(m)+1)}{2} d_y(m) \equiv T(m,q)d_y(m) \end{aligned} \tag{4}$$

so that

$$\begin{aligned} F_s(m) = &\sum_{p=1}^{N_x(m)} \sum_{q=1}^{N_y(m)} W(m,p,q) \\ &\times \exp\left[jk(P(m,p)d_x(m)u_m + T(m,q)d_y(m)v_m)\right]. \end{aligned} \tag{5}$$

The total distributed array pattern is obtained by including the array factor constructed from the centers of each subarray

$$F_t = \sum_{m=1}^{N_s} F_s(m) \exp\left[jk\left(x_s(m)u + y_s(m)v + z_s(m)w\right)\right]. \tag{6}$$

To complete the expression for the pattern, an element factor must be added. In the local subarray coordinates (θ_m, ϕ_m), the element factor $\vec{S}$ for subarray *m* can be expressed as

$$\vec{S}(m,\theta_m,\phi_m) = S_\theta(m,\theta_m,\phi_m)\hat{\theta}_m + S_\phi(m,\theta_m,\phi_m)\hat{\phi}_m. \tag{7}$$

This allows for the possibility that elements are different for each subarray, which generally would not be the case. The final, most general expression for the total array pattern is

$$\begin{aligned} \vec{F}_t(\theta,\phi) = &\sum_{m=1}^{N_s} F_s(m)\ \vec{S}(m,u_m,v_m) \\ &\times \exp\left\{jk\left[x_s(m)(u-u_s) + y_s(m)(v-v_s)\right.\right. \\ &\left.\left. + z_s(m)(w-w_s)\right]\right\}. \end{aligned} \tag{8}$$

The normalized power pattern is computed by

$$P_{\text{norm}}(\theta,\phi) = \frac{\left|\vec{F}_t(\theta,\phi)\right|^2}{\left|\vec{F}_t(\theta,\phi)\right|^2_{\max}} = \frac{\vec{F}_t(\theta,\phi) \bullet \vec{F}_t(\theta,\phi)^*}{\left|\vec{F}_t(\theta,\phi)\right|^2_{\max}} \tag{9}$$

where * is complex conjugation. For the remainder of the paper, we consider only isotropic elements and neglect the element factor.

The general formulas of (5) and (6) can be reduced to closed form for a periodic planar rectangular array of subarrays with uniform weights. The index *m* can be dropped from the subarray quantities if all subarrays are identical. The subscript *m* can also be dropped from the direction cosines because all subarrays are aligned with the global coordinate system. The final formulas contain the familiar uniform array functions found in [3] and [4].

Note that when receiving, the exponential factor in (5) would be obtained from the element baseband in-phase (I) and quadrature (Q) samples

$$\begin{aligned} I(m,p,q) + jQ(m,p,q) \equiv &\exp\left[jk(P(m,p)d_x(m)u_m\right. \\ &\left. + T(m,q)d_y(m)v_m)\right]. \end{aligned} \tag{10}$$

In a digital beamforming approach, the weights are applied in the processing to obtain the array response. In the virtual filling technique, virtual elements are added to the summation in (5) based on estimates of the I and Q values at their locations. As

will be shown in Section V, the response of a contiguous array can be duplicated.

III. GL Suppression for DDSAs

A. Conventional Methods

If the element spacing is small enough so that individual subarray GLs do not occur for any scan angle, then any GLs that occur are due to the gaps between the subarrays in the rectangular grid (i.e., the lattice GLs, also called construction GLs). Some of the conventional (traditional) GL suppression techniques are as follows.

1) Placement of Element Pattern Nulls: The array can incorporate an element that has nulls at the locations of the GLs [5].

2) Subarray Lattice Selection: Arrays can employ nonrectangular periodic lattice configurations [6].

3) Placement of Subarray Nulls: One can select the subarray spacing and size so that subarray pattern nulls fall at the GL locations [7].

4) Perturbations in the Geometry: Minor changes in the geometry such as rotation and tilt of the subarrays can be used to reduce (but not eliminate) the GLs [8], [9].

5) Multiplicative Beamforming: Multiplicative beamforming on the receiving side has been employed in [10]–[12]. The GLs can be suppressed by multiplication of the main and auxiliary array outputs.

6) Aperiodic or Random Subarray Sizes: Random subarraying has been proposed for contiguous array antennas to reduce the GLs due to the subarray steering or when the phase center distances between subarrays are too large [13], [14].

7) Aperiodic or Random Displacement: An aperiodic or random array has no GLs because there is no strong periodicity [15]–[17]. Taken to the extreme, this would be an array where the subarray locations are completely random (subject to any nonoverlapping constraints). For the DDSA case, aperiodic or random displacement of identical subarrays is an option for lowering the GLs. Most practical applications do not allow for randomly distributed locations. One exception would be a "randomly thinned" array of subarrays because it is deployed over a well-defined area.

B. Virtual Filling Method

Virtual filling is a digital processing method that can only be used on the receiving side [18]. The idea is to fill the gaps of a DDSA with virtual elements in the processing so that the synthesized pattern has no GLs, and amplitude tapering for sidelobe control can be applied [19]. The response of a contiguous array can be duplicated in a number of directions limited by the total number of elements. The directions of interest would normally be those of the desired signal (main beam) and interference or clutter (sidelobes).

The procedure can be viewed as an interpolation of the incident wave phases at the locations of the virtual elements from measurements of the phases at the real elements. Multiple time samples (snapshots) are taken at the real elements and virtual element phases estimated from the direction-of-arrival (DOA) information. No hardware is associated with the virtual elements. Equations (5) and (6) still hold, although terms are added for the virtual elements.

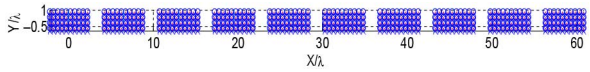

Fig. 2. Physical layout of a periodic distributed linear array composed of 10 identical planar subarrays whose centers are equally spaced. The gap between subarrays is 1.5λ.

The modified matrix pencil method is ideally suited for this direction finding problem [20]. In [19], the modified matrix pencil method has been extended to handle the problem of multiple subarrays for both single and multiple snapshots. After filling the gaps between subarrays virtually, the "filled" array can be treated as contiguous, and therefore, some advantages that come with a larger contiguous aperture array are obtained. In particular, the strong array response to signals received in the GLs is suppressed and sidelobe tapers can be applied to increase the signal-to-clutter ratio [21]. The effectiveness of this method depends on the SNR and DOA errors, which are addressed briefly in Section VII.

C. Combined Solution for Two-Way GL Suppression

The conventional solutions provide moderate (several dB) of GL suppression [14], [22]. Since the virtual filling method is applicable when receiving only, the combination of a conventional solution on the transmitting side, such as random displacements and sizes, in conjunction with digital beamforming and virtual filling for the receiving side is proposed. Improvement in the two-way pattern, in terms of lower sidelobes and GLs, is possible due to the pattern multiplication.

IV. Conventional Method for Transmitting Side

For attacking the GL problem on the transmitting side, introducing randomness is one of the possible approaches. We consider subarrays with random displacements and sizes. Simulation results shown in this section are the ones with the lowest GLs based on 100 Monte Carlo trials of which the maximum GLs are identified for all trials. It should be noted that for other numbers of trials, the best arrangement might be different.

As an example, suppose we would like to design a DDSA where each subarray is a periodic array with 10 elements along x and 4 elements along y, with an element spacing of $\lambda/2$ in both dimensions. Subarrays are separated by gaps of 1.5λ. In Figs. 2 and 3, the physical layout and radiation pattern can be seen, respectively. GLs occur due to the periodic gaps between subarrays.

A. Random Subarray Displacement and Sizes

As a first step in reducing GLs, we add random positions for each subarray in addition to their random sizes as shown in Fig. 4. As can be seen in Fig. 5, the peak GL level has been lowered by about 6.5 dB by randomization.

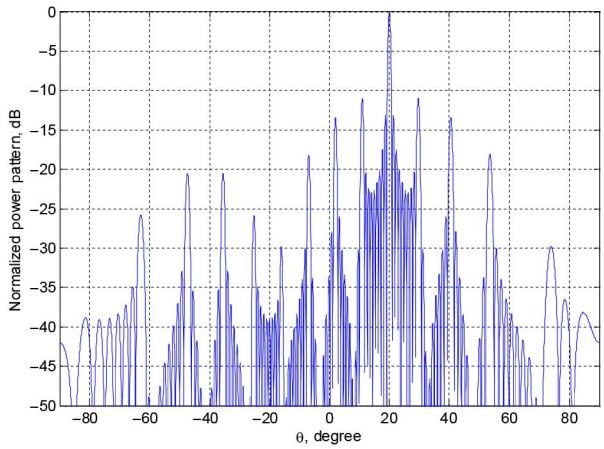

Fig. 3. Scanned radiation pattern of the periodic distributed subarray antenna shown in Fig. 2.

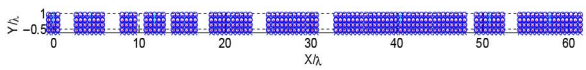

Fig. 4. Physical layout of the array with random subarray sizes and random subarray locations.

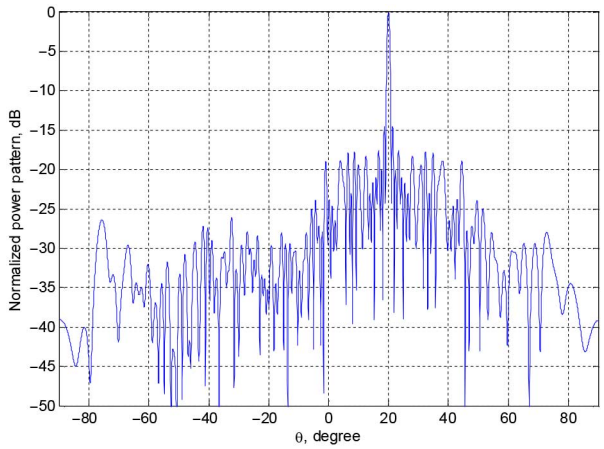

Fig. 5. Radiation pattern of the array shown in Fig. 4 scanned to 20°.

V. Combining Conventional Methods and the Virtual Filling Method

A. Introduction

In [19], we proposed the virtual filling method on the receiving side to mimic a contiguous array pattern, and therefore, a sidelobe taper can be applied to lower the sidelobes. The virtual filling method cannot be used on the transmitting side, and the GLs from a DDSA on the transmitting side can only be addressed with traditional methods as discussed in Section III.

For the purpose of illustration, we choose random subarray sizes with fixed subarray gaps for the transmitting model for two reasons. First, since the gaps between subarrays are fixed, it is much easier to implement this configuration in practice compared to arrangements with random gaps. Second, with random subarray sizes and fixed subarray gaps, the subarray phase centers are actually randomized and GLs are partially suppressed.

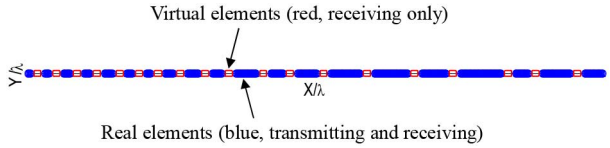

Fig. 6. The transmitting DDSA model with real elements (in blue) and the receiving DDSA model with real and virtual elements (in blue and red, respectively).

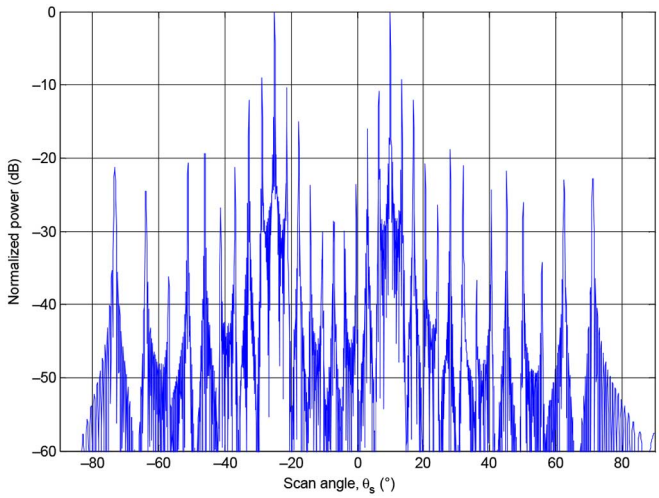

Fig. 7. Periodic DDSA receiving pattern for equal amplitude signals from 10° and −25°.

B. Simulation Results

A random-sized 20-subarray DDSA with number of elements of 6, 8, 12, 10, 14, 10, 8, 14, 18, 16, 33, 21, 31, 47, 53, 39, 65, 21, 45, 29 was first chosen on the basis of the lowest GL level from 100 Monte Carlo simulation trials that randomly assigned the number of elements of each subarray under the constraint that the total number of elements in the DDSA was 500. Element spacings are 0.48λ, and spacings between subarrays are 4.8λ. The DDSA model is shown in Fig. 6.

Two signals of equal power coming in from 10° and -25° relative to broadside are used for this simulation. One of these represents the desired signal from a point target and the other an undesired signal such as clutter return from a hill or structure. In a real scenario, the amplitudes and phases will be determined by target radar cross section, clutter cross section, ranges, transmitting antenna gain values, etc., but first we consider a simple case of equal magnitudes and noncoherent phases (arbitrarily chosen as $\pi/5$ and $-4\pi/5$) for the two signals.

The transmitting pattern has a Taylor amplitude taper with parameters $\overline{n} = 5$, $\mathrm{SLL} = -20$ dB. On the receiving side, thermal noise with an SNR of 6 dB is added to the I and Q components at each real element.

A baseline receiving pattern of the periodic 20-subarray DDSA (25 elements in each subarray) is shown in Fig. 7, for reference. The plot gives the response of the array in the main

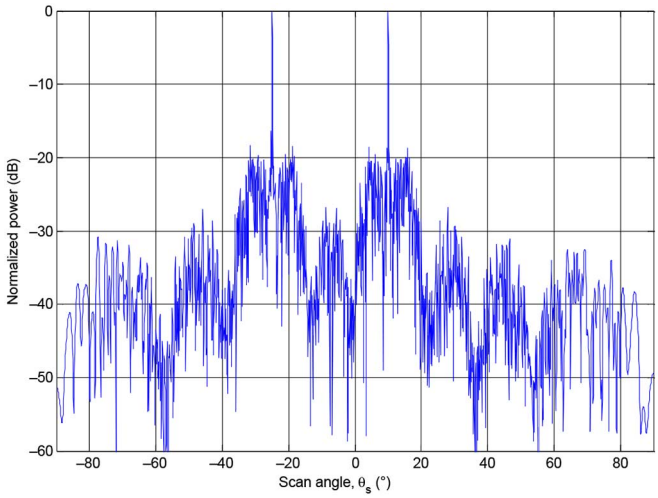

Fig. 8. Receiving pattern for a DDSA with random subarray sizes and equal amplitude signals from 10° and -25°.

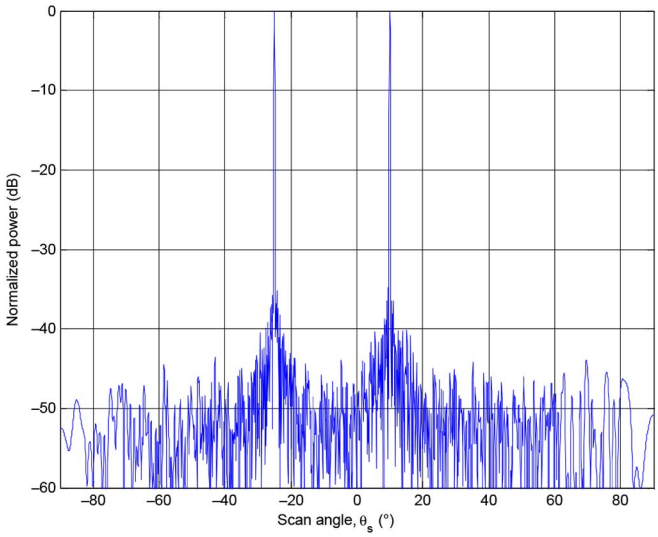

Fig. 9. DDSA with random subarray sizes and virtual filling of the receiving array using 100 snapshots for equal signals from 10° and -25°. A 35-dB Taylor distribution was applied and the element SNR is 6 dB.

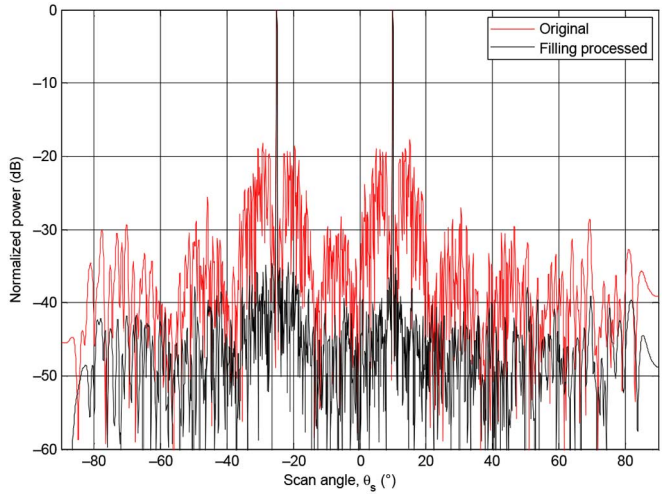

Fig. 10. DDSA with random subarray sizes and virtual filling of the receiving array using 30 snapshots for equal signals from 10° and -25°. A 35-dB Taylor distribution was applied and the element SNR is 6 dB.

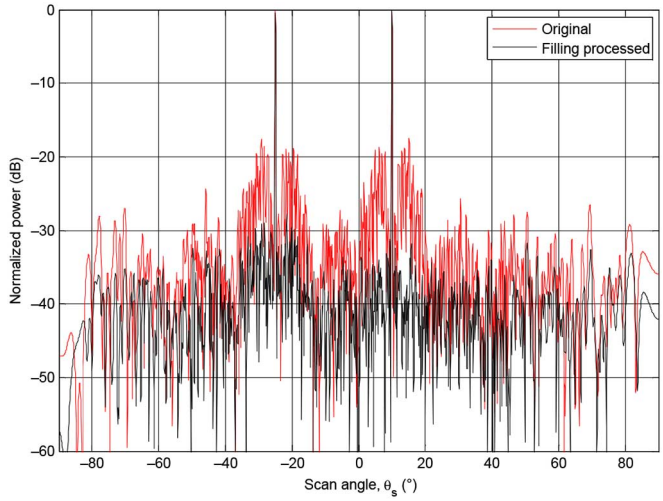

Fig. 11. DDSA with random subarray sizes and virtual filling of the receiving array using 30 snapshots for equal signals from 10° and -25°. A 35-dB Taylor distribution was applied and the element SNR is 0 dB.

beam scan direction θ_s when signals are incident from the specified directions. A conventional filled array with low sidelobes has large responses that occur in the directions of the signals, whether desired or not, because the main beam is pointed in their direction. A distributed array with gaps has large responses not only in the directions of the signals when they are in the mainbeam, but also when the signals are in the GL directions.

The receiving pattern of the random 20-subarray case is shown in Fig. 8. The randomness has lowered the GLs but also increased the average sidelobe level. In Fig. 9, the sidelobe level of the receiving array has been lowered by virtually filling the gaps between subarrays and applying a Taylor amplitude taper ($\overline{n} = 5$, SLL $= -35$ dB). The virtual elements used to fill the gaps were estimated from 100 noisy snapshots (time samples) of receiving signals.

To illustrate the effectiveness of the virtual method, the array responses for varying element SNRs, incoming signal strengths, and number of snapshots are shown in Figs. 10–14. The "original array" is the pattern using the real elements. The "filling processed" pattern results after the virtual filling processing. Comparing Figs. 9 and 10 and Figs. 11 and 12 illustrates the dependence of the response on the number of snapshots (100 vs. 30). A comparison of Figs. 9 and 12 and Figs. 10 and 11 gives an indication of how the response varies with element SNR. The patterns in Figs. 13 and 14 show the array responses for unequal signal amplitudes.

Comparisons verify that the virtually filled distributed array has the same behavior as an array with no GLs and that amplitude tapering can be applied. The processing tradeoffs are also evident. The SNR per element can be traded off with number of snapshots. Increasing the number of snapshots increases the required observation time, and therefore, delays the beamforming calculation, which in turn introduces latency into the system.

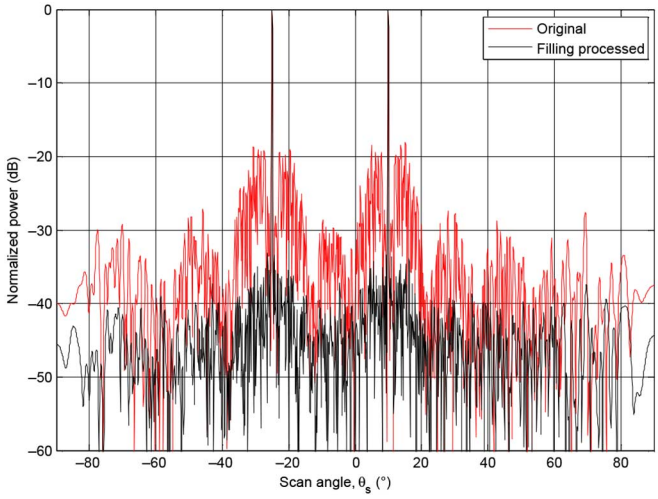

Fig. 12. DDSA with random subarray sizes and virtual filling of the receiving array using 100 snapshots for equal signals from 10° and -25°. A 35-dB Taylor distribution was applied and 0-dB element SNR.

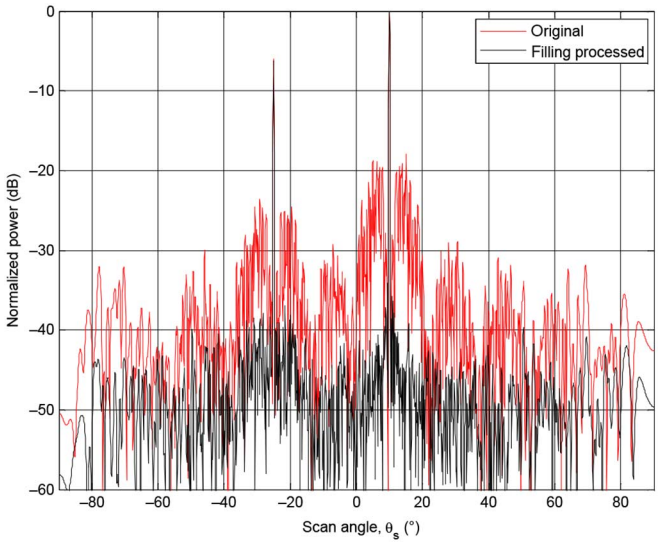

Fig. 13. DDSA with random subarray sizes and virtual filling of the receiving array using 30 snapshots for 6-dB unequal signals from 10° and -25°. A 35-dB Taylor distribution was applied and the element SNR is 6 dB.

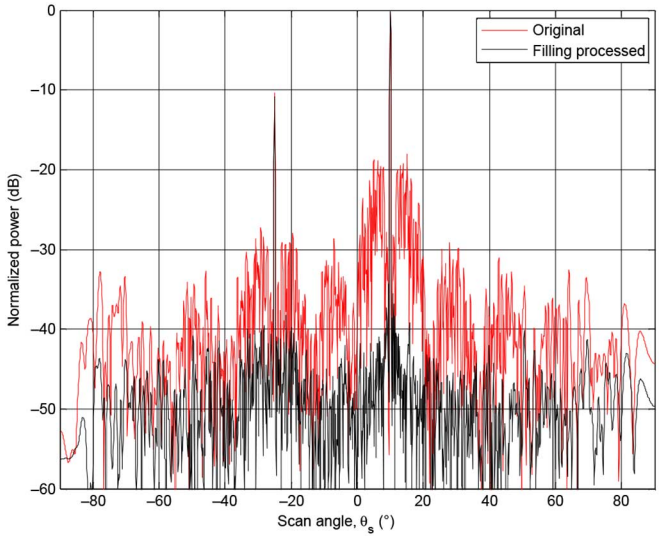

Fig. 14. DDSA with random subarray sizes and virtual filling of the receiving array using 30 snapshots for 10-dB unequal signals from 10° and -25°. A 35-dB Taylor distribution was applied and the element SNR is 6 dB.

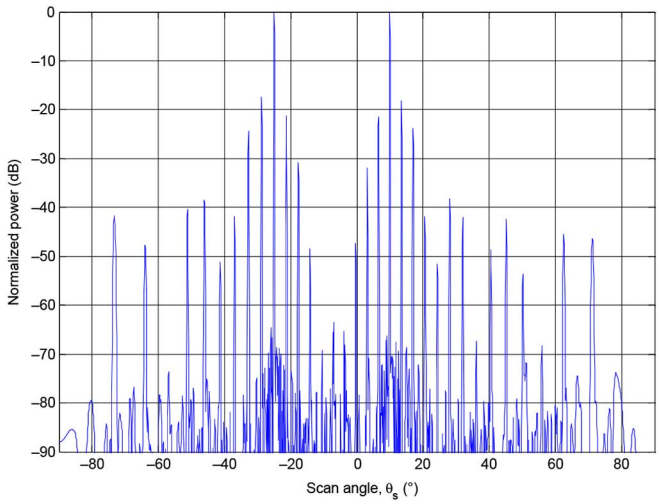

Fig. 15. Periodic DDSA two-way pattern for equal amplitude signals from 10° and -25°.

VI. Two-Way Pattern Design

A. Approach

Applying pattern multiplication, the normalized two-way pattern is defined as

$$F_{norm_{2way}}(\theta_s,\phi) = F_{norm_{Tx}}(\theta_s,\phi) \times F_{norm_{Rx}}(\theta_s,\phi) \quad (11)$$

where $F_{norm_{Tx}}(\theta_s,\phi)$ is the normalized pattern of the transmitting DDSA array, and $F_{norm_{Rx}}(\theta_s,\phi)$ is the normalized pattern of receiving DDSA array. Both beams are scanned to the same angle θ_s. Using the two-way pattern multiplication approach, we shall see that the remaining DDSA transmitting GLs can be reduced by the pattern of the DDSA receiving array.

Suppose we use a combination of random subarray size and locations for the transmitting DDSA and apply virtual filling for the receiving DDSA illustrated in Fig. 6. Because of the same aperture size, both transmitting and receiving patterns possess the same main beamwidth. The low sidelobe attribute of the receiving pattern can significantly reduce the GLs of the transmitting pattern after the multiplication has been done.

B. Simulation Results

For comparison purposes, a two-way pattern of the periodic DDSA is shown in Fig. 15. The two-way pattern shown in Fig. 16 is obtained from the transmitting pattern and the filled receiving pattern. The relative sidelobe level has gone down to less than -50 dB without affecting the mainbeam.

Using the combination of random sizes and locations when transmitting, and the virtual filling method when receiving, an improved two-way pattern with an ultralow sidelobe level is obtained.

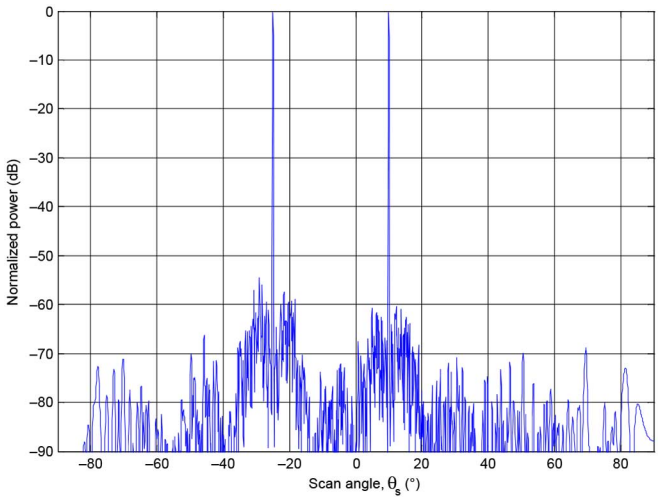

Fig. 16. Two-way scanning pattern of a DDSA with random subarray sizes and virtual filling of the receiving array using 30 snapshots for equal amplitude signals from 10° and -25°. Taylor distributions were applied and the element SNR is 6 dB.

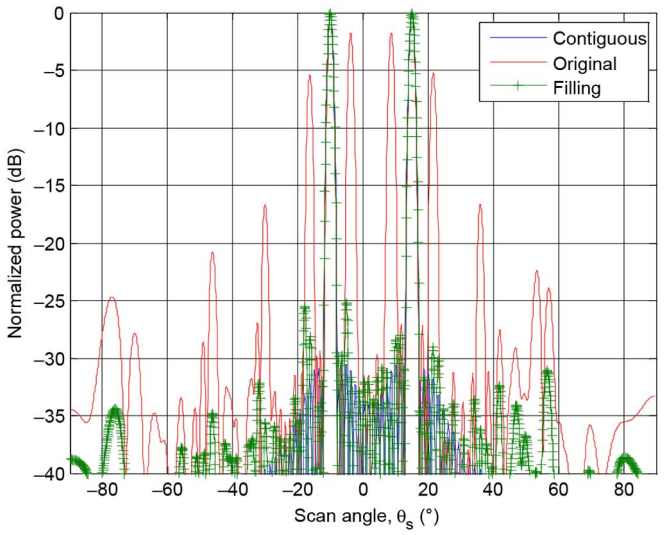

Fig. 17. Performance comparison of contiguous, original DDSA, and virtual filled array. Assuming no fixed errors and with 6-dB SNR at each element. Taylor amplitude taper has been applied. Equal amplitude signals from 10° and -25°.

VII. Data Sampling, Calibration, Noise and Errors

There are many conceivable radar architectures that could incorporate subarrays with virtual elements, and since modern radars are tending toward completely digital, this virtual approach might be only one of several modes of operation. Although the proposed antenna system does not rely on combined transmit and receive modules at each element, the technology to accomplish this has been demonstrated [23], and all of the necessary components are commercially available in the wireless frequency bands.

The data sampling requirements are dependent on the specific radar (carrier frequency, waveform parameters, bandwidth, type of demodulation scheme used, etc.) A system level simulation of the radar is required to optimize the antenna parameters for a specific radar function.

The effectiveness of the virtual method is determined by the accuracy of the signal DOA estimates used to find the virtual element phases. For a practical application, noise and errors cause degradation of the DOA estimates. Some types of error, such as those due to manufacturing imperfections, mutual coupling, quantization, and calibration errors [24], [25], can be measured or predicted in advance and possibly be compensated for by adjustment of the array weights [26], [27]. Thermal noise appears in almost all receivers and is commonly modeled as random from sample to sample. Here we will consider a combination of the two types of error. One is a fixed error that is random from element to element, but unchanging in time. The second is random from sample to sample (i.e., between snapshots).

We model the thermal noise at the element level by specifying the element SNR. Low-noise amplifiers at each element can be used to increase the element level SNR.

As an example, we use a five-subarray DDSA to examine the effects of fixed errors on the DOA estimation and virtual filling method. Each subarray comprised 10 elements with element spacing equal to 0.45λ. Subarray center distances are 10λ.

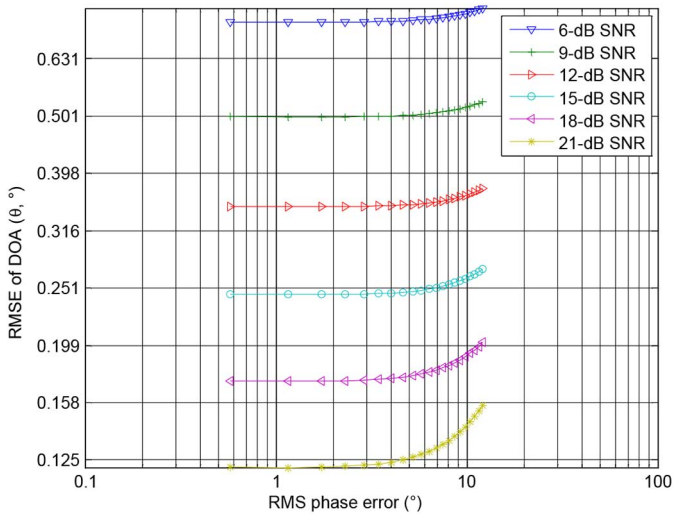

Fig. 18. RMSE of DOA versus rms phase errors from 0° to 12.1° for different element SNRs.

Fixed errors are uniformly distributed from -21° to 21° (root-mean-square [rms] error [RMSE] values from 0° to 12.1°), and the SNR is varied from 6 to 21 dB at each element. We consider two equal amplitude signals impinging on the DDSA from DOAs of -10° and 15° relative to broadside. The receiving patterns for 6-dB element SNR for the ideal contiguous array of the same aperture size as the DDSA, the original DDSA, and the virtually filled one are compared in Fig. 17. There is about 20 dB of improvement in GL and sidelobe suppression observed after applying the virtual filling method.

A DOA error leads to incorrect weights for the virtual elements, resulting in degraded GL suppression and SL reduction. In order to quantify the effect of fixed errors on the DOA estimation, a plot that compares the RMSE of the DOA versus rms phase error for different SNR levels is shown in Fig. 18. The

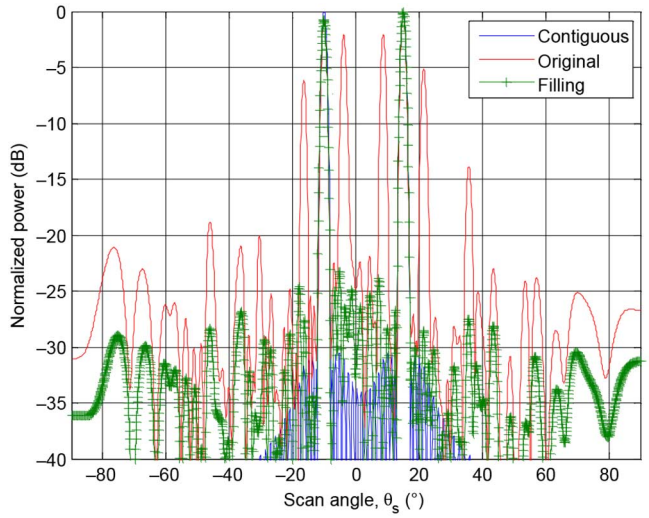

Fig. 19. Pattern comparison of contiguous, original DDSA, and virtual filled DDSA for 21° fixed error and with 6-dB SNR at each element. Taylor amplitude taper ($\overline{n} = 5$, SLL $= -30$ dB) has been applied. Plots are normalized to the contiguous error free case in Fig. 17.

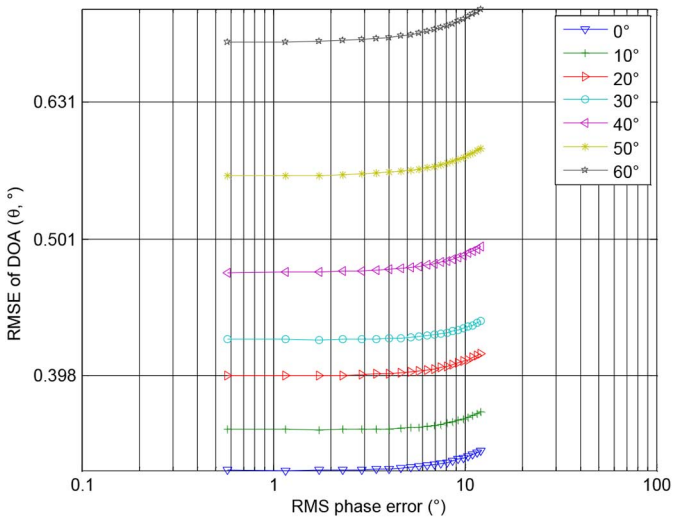

Fig. 20. RMSE of DOA versus rms phase errors from 0° to 12.1° and 6-dB SNR per element for different signal angles.

formula used to calculate the average RMSE of the DOA for K signals is

$$RMSE = \sqrt{\frac{\sum_{r=1}^{K}\left[\left(\hat{\theta}_r - \theta_r\right)^2\right]}{K}} \tag{12}$$

where $\hat{\theta}_r$ is the estimated angle, and θ_r is the true angle of signal r. Two conclusions can be made.

1) The most efficient way to improve the RMSE of the DOA is to increase the SNR at each element. Alternately, more shapshots can be collected.
2) For rms phase errors less than 6° which correspond to a fixed error of $-10.5°$ to $10.5°$, the effect on DOA estimation can be ignored for all SNRs considered.

In cases where the fixed errors can be compensated for by precalculation or premeasurement, there will still be some residual error after correction. We consider residual phase errors up to 21° and examine how they degrade the radiation pattern. Fig. 19 has a plot of the pattern of the worst case (21° fixed error) for a 6-dB SNR. Comparing Fig. 19 with Fig. 17, we see that the effect of the fixed error on the receiving pattern is to increase the sidelobe level and lower the main beam by 0.6 dB.

We also consider the effect of signal angle on the RMSE of the DOA with fixed errors uniformly distributed between $-21°$ and 21° and 6-dB SNR per element. As can be seen in Fig. 20, because the projected aperture area decreases at large signal angles, the RMSE of the DOA is increased.

VIII. Summary and Conclusion

This paper has focused on the fundamental issues of GL suppression and error effects for DDSAs. In a general sense, using more elements in an array system can potentially increase the array gain when transmitting, and increase the output SNR when receiving. Often the mechanical, structural, and operational limitations discussed in Section I can prohibit the use of a large contiguous array on a platform. The idea of using separated arrays that together form a DDSA is a potential solution to this dilemma. The critical issues that must be addressed are calibration, time and frequency synchronization, error correction, and GLs.

This study examined a combined approach to suppress the GLs of a DDSA on both the transmitting and receiving sides. Several conventional methods for GL suppression were mentioned in Section III. By combining several GL reduction methods, such as random sizes and locations, the GLs can be reduced more than when using any one of the methods individually. Potential disadvantages, such as polarization loss, hardware complexity, gain loss and limited suppression ability for large separations, restrict the use of the methods, and therefore, tradeoffs need to be made accordingly.

Filling gaps between arrays with virtual elements for the purpose of receiving processing allows a synthesized antenna response that duplicates a contiguous array in a number of directions that is limited by the total number of elements used in the processing. The synthesized response has no GLs and can have low sidelobes, as seen in Section V. As a first step in the virtual processing, the signal amplitudes, phases, and DOAs must be extracted from the real element I and Q samples. These data are used generate I and Q samples that would be provided by virtual elements filling the gaps between distributed subarrays. Low sidelobes, interference rejection, and an improved two-way pattern with an ultralow sidelobe level were demonstrated for the virtual processed DDSA.

References

[1] R. C. Heimiller, J. E. Belyea, and P. G. Tomlinson, "Distributed array radar," *IEEE Trans. Aerosp. Electron. Syst.*, vol. 19, no. 6, pp. 831–839, Nov. 1983.
[2] K. Nishizawa, K. Hirata, S.-I. Kan, H. Miyashita, and S. Makino, "Experimental investigations into grating lobe suppression in distributed array antennas," in *Proc. Int. Symp. Antennas Propag.*, Nov. 2006, p. 201.
[3] W. L. Stutzman and G. A. Thiele, *Antenna Theory and Design*. Hoboken, NJ, USA: Wiley, 2012.

[4] R. Mailloux, *Phased Array Antenna Handbook*, 2nd ed. Norwood, MA, USA: Artech House, 2005.
[5] F. J. Pompei and S.-C. Wooh, "Phased array element shapes for suppressing grating lobes," *J. Acoust. Soc. Amer.*, vol. 111, pp. 2040–2048, 2002.
[6] A. J. Zaman, E. Rho, R. Q. Lee, and M. L. Zimmerman, "Grating lobe characteristics of a hexagonal array of subarrays," in *Proc. Antennas Propag. Soc. Int. Symp.*, 1991, vol. 2, pp. 1140–1143.
[7] C.-H. Lin, "Distributed subarray antennas for multifunction phased-array radar," M.S. thesis, Naval Postgraduate Sch., Monterey, CA, USA, 2003.
[8] V. D. Agrawal, "Grating-lobe suppression in phased arrays by subarray rotation," *Proc. IEEE*, vol. 66, no. 3, pp. 347–349, Mar. 1978.
[9] Y. V. Krivosheev and A. V. Shishlov, "Grating lobe suppression in phased arrays composed of identical or similar subarrays," in *Proc. IEEE Int. Symp. Phased Array Syst. Technol.*, Oct. 2010, pp. 724–730.
[10] D. E. N. Davies and C. R. Ward, "Low sidelobe patterns from thinned arrays using multiplicative processing," *IEE Proc. F. Commun. Radar Signal Process.*, vol. 127, no. 1, p. 9, Feb. 1980.
[11] A. Ksienski, "Multiplicative processing antenna systems for radar applications," *Radio Electron. Eng.*, vol. 29, pp. 53–67, 1965.
[12] L. E. Miller and J. S. Lee, "Capabilities of multiplicative array processors as signal detector and bearing estimator," Defense Tech. Inf. Center, Final Rep., Dec. 1974.
[13] R. Willey, "Space tapering of linear and planar arrays," *IRE Trans. Antennas Propag.*, vol. 10, no. 4, pp. 369–377, Jul. 1962.
[14] W. C. Barott and P. G. Steffes, "Grating lobe reduction in aperiodic linear arrays of physically large antennas," *IEEE Antennas Wireless Propag. Lett.*, vol. 8, pp. 406–408, Sep. 2009.
[15] Y. Lo, "A mathematical theory of antenna arrays with randomly spaced elements," *IEEE Trans. Antennas Propag.*, vol. 12, no. 3, pp. 257–268, May 1964.
[16] A. P. Goffer, M. Kam, and P. R. Herczfeld, "Design of phased arrays in terms of random subarrays," *IEEE Trans. Antennas Propag.*, vol. 42, no. 6, pp. 820–826, Jun. 1994.
[17] A. P. Goffer, M. Kam, and P. R. Herczfeld, "Wide-bandwidth phased arrays using random subarraying," in *Proc. 20th Eur. Microw. Conf.*, Sep. 1990, vol. 1, pp. 241–246.
[18] W. Chen, X. Xu, S. Wen, and Z. Cao, "Super-resolution direction finding with far-separated subarrays using virtual array elements," *IET Radar Sonar Navigat.*, vol. 5, no. 8, pp. 824–834, Oct. 2011.
[19] B. Feng and D. C. Jenn, "Grating lobe suppression for distributed digital subarrays using virtual filling," *IEEE Antennas Wireless Propag. Lett.*, vol. 12, pp. 1323–1326, Oct. 2013.
[20] V. D. Karira and S. R. Katuri, "Application of a modified matrix pencil method for direction of arrival and time of arrival estimation: Scenarios based on the number of antenna elements, signal to noise ratio (SNR), and spread," in *Proc. Annu. IEEE India Conf. (INDICON)*, Dec. 2011, pp. 1–4.
[21] W. K. Burger, "Sidelobe forming for ground clutter and jammer suppression for airborne active array radar," in *Proc. IEEE Int. Symp. Phased Array Syst. Technol.*, Oct. 2003, pp. 271–276.
[22] W. Hao, F. Da-Gang, and Y. L. Chow, "Grating lobe reduction in a phased array of limited scanning," *IEEE Trans. Antennas Propag.*, vol. 56, no. 6, pp. 1581–1586, Jun. 2008.
[23] W. Chappell. (2002, Aug. 3). *Digital Array Radar Technology for Low Cost Radar*, DARPA/MTO [Online]. Available: http://www.ofcm.noaa.gov/wg-mpar/meetings/2012-01/06%20DARPA.pdf
[24] C. M. Schmid, S. Schuster, R. Feger, and A. Stelzer, "On the effects of calibration errors and mutual coupling on the beam pattern of an antenna array," *IEEE Trans. Antennas Propag.*, vol. 61, no. 8, pp. 4063–4072, Aug. 2013.
[25] M. Lange, "Impact of statistical errors on active phased-array antenna performance," in *Proc. IEEE Mil. Commun. Conf.*, 2007, pp. 1–5.
[26] B. Svensson, M. Lanne, and J. Wingard, "Element position error compensation in active phased array antennas," in *Proc. 4th Eur. Conf. Antennas Propag. (EuCAP)*, 2010, pp. 1–3.
[27] U. V. Buch, "Analysis of mutual coupling in adaptive antennas and techniques used for compensation," in *Proc. 9th Int. Conf. Telecommun. Mod. Satell. Cable Broadcast. Serv. (TELSIKS'09)*, 2009, pp. 368–371.

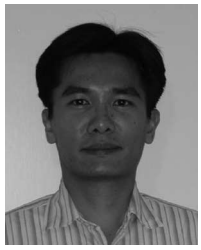

Bo-Kai Feng (S'10–M'14) received the Ph.D. degree in electrical engineering from the Naval Postgraduate School, Monterey, CA, USA, in 2013, the B.S. degree in materials science and engineering from the Chung Cheng Institute of Technology, Longtan, Taiwan, in 1999, and an M.S. degree in system engineering from the Naval Postgraduate School in 2006.

In 2002, he joined the Material and Electro-Optical Research Division, Chung-Shan Institute of Science and Technology, Longtan, Taiwan, where he was involved in the research of laser-related applications. He is a Senior Engineer of Electro-Optical Systems with the National Chung-Shan Institute of Science and Technology, Longtan, Taiwan.

David C. Jenn (M'76–SM'93) received the B.S. degree in electrical engineering from the University of Wisconsin—Milwaukee, Milwaukee, WI, USA, in 1975, the M.S. degree in electrical engineering from the Ohio State University, Columbus, OH, USA, in 1976, and the Ph.D. degree in electrical engineering from the University of Southern California, Los Angeles, CA, USA, in 1987.

From 1976 to 1978, he was with McDonnell Douglas Astronautics Co., where he was involved in the design of small arrays and radomes for missiles and spacecraft. He also worked on the radar altimeter and antennas for various cruise missiles. In 1978, he joined Hughes Aircraft Co., where he concentrated on the design and analysis of high-performance-phased array antennas for radar and communication systems, and radar cross-section analysis. During this time, he contributed to the development and upgrades of the AN/TPQ-37 Firefinder radar, and the Hughes Air Defense Radar (HADR). In 1990, he joined the Department of Electrical and Computer Engineering, Naval Postgraduate School, Monterey, CA, USA, where he is currently a Professor. He is the Faculty Director of the NPS Microwave and Antenna Laboratory and author of the book, *Radar and Laser Cross Section Engineering*. He has developed and taught courses in the areas of antennas, propagation, microwave devices, radar cross section, and communications systems. While at NPS, he has advised over 140 thesis students from more than 20 countries. His research interests include a wide range of topics in electromagnetics including, radar systems, microwave circuits and devices, antennas, and scattering and propagation.